JOURNAL OF GEOPHYSICAL RESEARCH, VOL. 103, NO. D11, PAGES 13,519–13,529, JUNE 20, 1998

Photochemistry of O_3 and related compounds over southern Nova Scotia

Lawrence I. Kleinman, Peter H. Daum, Jai H. Lee, Yin-Nan Lee,
Judith Weinstein-Lloyd, and Stephen R. Springston

Department of Applied Science, Environmental Chemistry Division, Brookhaven National Laboratory
Upton, New York

Martin Buhr and B. Thomas Jobson

Aeronomy Laboratory, National Oceanic and Atmospheric Administration, Boulder, Colorado

Abstract. Photochemical model calculations have been performed for air masses encountered by the National Research Council's Twin Otter aircraft during the 1993 summer North Atlantic Regional Experiment (NARE) intensive. These calculations use observed values of O_3, NO_y, CO, and hydrocarbons as constraints. NO is determined using the ratio NO/NO_y measured from the National Center for Atmospheric Research King Air under comparable circumstances. Measurements over coastal locations indicate photochemically aged air masses with relatively low concentrations of NO and an OH reactivity that is dominated by CO and CH_4. Samples over land have higher NO and an OH reactivity that is dominated by isoprene. Ozone production rates and H_2O_2 concentrations are analyzed using radical budget arguments that are applicable to low NO_x conditions. The ozone production rate, $P(O_3)$, is predicted to be proportional to $Q^{1/2}[NO]$, where Q is the production rate for free radicals. This relation explains 99% of the variance in $P(O_3)$. Over 90% of the variance is explained by [NO] alone. $P(O_3)$ in the coastal samples is about a factor of 4 lower than previous estimates for the eastern United States. This is a consequence of low [NO] in the air masses that are advected to Nova Scotia.

1. Introduction

An extensive set of chemical measurements were made at the surface and in the air over southern Nova Scotia, the Gulf of Maine, and adjoining areas of the North Atlantic Ocean during the 1993 summer North Atlantic Regional Experiment (NARE) intensive. As part of this experiment, the National Research Council (NRC) of Canada's Twin Otter was deployed in Yarmouth, Nova Scotia. A total of 48 flights were conducted, consisting primarily of vertical profiles and short traverses over the surface sampling site in Chebogue Point and nearby Atlantic Ocean. Results from the Twin Otter are reported in a series of papers covering wind measurements [*Angevine and MacPherson*, 1995], export of O_3 and other pollutants in the North American plume [*Banic et al.*, 1996], aerosol composition [*Chylek et al.*, 1996; *Li et al.*, 1996], O_3 and its precursors [*Kleinman et al.*, 1996a,b], carbonyl compounds [*Lee et al.*, 1996], and cloud chemical and microphysical properties [*Leaitch et al.*, 1996].

The Twin Otter aircraft encountered a wide range of pollutant conditions over southern Nova Scotia. A prominent feature of the observations (which is also shown in the data sets collected from the Department of Energy (DOE) G-1 [*Daum et al.*, 1996] and NCAR King Air aircraft [*Buhr et al.*, 1996] is that elevated concentrations of O_3 and other anthropogenic pollutants were observed in well defined layers usually located a few hundred meters above the ocean surface. These layers represent transport of boundary layer air from the North American mainland. Under other flow conditions, southern Nova Scotia can be exposed to much cleaner air with a marine boundary layer origin. At higher altitude, in the free troposphere, high O_3 layers also were observed, sometimes occurring in conjunction with other anthropogenic pollutants and sometimes appearing to be of natural origin.

The NARE measurement campaign resulted in a detailed picture of O_3, other oxidants, and their precursors near southern Nova Scotia. The measurements by themselves, however, do not provide a time-dependent picture as they do not include the free radicals directly responsible for oxidation and O_3 formation, nor do they include the production and loss rates of O_3 and other oxidants. In this article we calculate these dynamic quantities using a photochemical box model in which concentrations of O_3, NO, CO, and hydrocarbons are constrained to their observed values. Most of the chemical and meteorological variables which define these calculations are reported by *Kleinman et al.* [1996 a,b]. We will refer to these studies as part 1 and part 2. The calculations yield (1) concentrations of species which were not measured, including OH, peroxy radicals, NO_2, and peroxyacetylnitrate (PAN); (2) concentrations of photochemical oxidation products (i.e., peroxides, HCHO and other carbonyl compounds) some of which can be compared with observations; (3) chemical rates of change, for example, rates of O_3 formation and destruction; and (4) reaction pathway information, for example, the sources and sinks of free radicals. Calculations have been performed for air parcels sampled by the Twin Otter

Paper number 97JD01484.

for which there is a "complete" complement of trace gas information. These calculations are a subset of the 105 hydrocarbon sample points described in part 2. For 82 of these samples, O_3, NO_y, and CO were also available. NO was determined from a combination of NO_y data from the Twin Otter and data on the ratio of NO to NO_y, observed under comparable circumstances from the King Air [*Buhr et al.*, 1996].

Similar steady state calculations have been applied to problems of deducing radical concentrations from observed stable compounds [*Cantrell et al.*, 1992, 1993; *Poppe et al.*, 1994; *Eisele et al.*, 1994], determining O_3 production rates [*Jacob et al.*, 1992; *Ridley et al.*, 1992; *Davis et al.*, 1993], testing photostationary state predictions [*Chameides et al.*, 1990; *Cantrell et al.*, 1992, 1993; *Liu et al.*, 1992; *Ridley et al.*, 1992; *Crawford et al.*, 1996], and determining concentrations of oxidation products for comparison with model predictions [*Liu et al.*, 1992; *Crawford et al.*, 1996; *Davis et al.* 1993].

Concentrations and rates are calculated using diurnal average photolysis rate constants and average values for the ratio NO to NO_y. This facilitates comparisons between calculations, but at the expense of providing sample specific predictions. A loss of specificity, however, is unavoidable because NO data were not available from the Twin Otter. Accordingly, we present our model predictions by groups; as a function of altitude and for data subsets defined by water vapor, O_3, and isoprene levels. Average vertical profiles are also calculated using data from the over-water portion of all 48 Twin Otter flights which removes some of the bias toward high pollutant episodes in the hydrocarbon sampling.

A central feature of the data set is that NO_x concentrations are relatively low even in air masses that have high concentrations of NO_y, O_3, and CO. In our presentation of model results we concentrate on features that reflect the low NO_x conditions in the aged photochemical mixtures that are advected to Nova Scotia. A radical budget equation is used to diagnosis the dependence of O_3 production rate on radical production rate and NO concentration. The dependence of H_2O_2 on radical production rate is shown along with a comparison between observed and calculated H_2O_2. We show that O_3 production rates are low in comparison to rates in a higher NO_x environment in the continental United States.

2. Model

Calculations are done with a box model in which a set of gas phase photochemical rate expressions is integrated for 40 daylight hours, a representative transport time for air advected to southern Nova Scotia. We used daytime average photolysis rate constants in order to generate a set of radical concentrations and rate predictions which could be compared from one calculation to another without large differences due to the varying times that samples were collected.

Chemical species are divided into two categories; constrained and calculated. Constrained species have concentrations which are fixed at their observed values. CH_4 is set to 1700 ppb. For each calculated compound there is a differential equation which gives the time rate of change of that compound in terms of rate constants and concentrations of calculated and constrained species. Initial concentrations for the calculated species are set at nominal clean-atmosphere values. Calculated species take varying amounts of time to come into equilibrium with the chemical mixture of constrained compounds. Free radicals (OH, HO_2, and RO_2) take seconds to minutes. NO_2 also reaches equilibrium in minutes. HCHO takes several hours to reach equilibrium. The slower reacting carbonyl compounds can take several days as can peroxides in some circumstances. Equilibrium is not reached for all compounds in 40 daylight hours, but a longer integration period would be unrealistic in view of back trajectory results.

Effects of varying the integration time between 0.4 and 100 hours were investigated for the over-water samples. Free radical concentrations and the production rate for O_3 decreased by 10-15% in the 0.4 hour calculation, which did not allow for the buildup of secondary oxidation products. An increase in the integration period to over 40 hours had little effect.

Calculations were done using a gas phase photochemical mechanism based on regional acid deposition model (RADM) II [*Stockwell et al.*, 1990] for the oxidation of anthropogenic hydrocarbons and based on the condensed mechanism of *Paulson and Seinfeld* [1992] for the oxidation of isoprene. These mechanisms contain a level of detail in the treatment of hydrocarbon oxidation that is commensurate with the level of detail in our observations. They were intended for use in a wide range of pollution conditions and therefore incorporate an explicit treatment for peroxy radical combination reactions which we expect to be important under the low NO_x conditions seen over southern Nova Scotia. Daytime average photolysis rate constants were calculated from the radiation code of *Madronich* [1987] taking into account the altitude of the calculation but using climatological values for aerosol extinction, O_3 column, and surface albedo. Zero cloud cover was assumed.

Several modifications to the published mechanisms of *Stockwell et al.* [1990] and *Paulson and Seinfeld* [1992] were dictated by our particular application. Species having negligible concentrations in the daytime (i.e., NO_3, N_2O_5, and HONO) were deleted. HNO_3 and $SO_4^=$ were also not considered as their concentration would be simply a linear function of integration time. PAN and analogues were calculated from their assumed equilibriums with NO_2 and peroxyacyl radicals. The alternative procedure of calculating PAN from a rate expression yields nearly identical concentrations except in the coldest samples.

Deposition losses were ignored in all calculations. Because of the constraints imposed by our observations, deposition can only have a significant effect on slowly forming oxidation products such as peroxides and the longer-lived carbonyls. Even for these compounds, we expect that dry deposition can be ignored in many cases. As described in part 1, most samples were taken over the Atlantic Ocean where a strong surface-based temperature inversion inhibited the downward transfer of pollutants. Scavenging by wet deposition is possible, but the effects would be limited to soluble substances, possibly only H_2O_2.

3. Measurements

The trace gas measurements taken from the Twin Otter have been described in detail in parts 1 and 2. NO and NO_y data from the King Air are presented by *Buhr et al.* [1996]. In this section we briefly review those measurements pertinent to the present calculations. We also present data on HC reactivity as observed from the Twin Otter.

3.1. Flight Patterns

The primary flight pattern of the Twin Otter consisted of vertical profiles and short horizontal traverses over southern Nova Scotia and the adjoining Atlantic Ocean. Vertical profiles

usually extended from below 100 m to either 3 or 5 km. There were also inland flights to Kejimkujik National Park and three flights dedicated to measurements over the city of Saint John, New Brunswick. Effects of nearby emission sources were seen during in-land flight segments but were rarely observed during flight segments over coastal Nova Scotia.

The King Air aircraft was stationed in Portland, Maine. Sampling was done near the North American mainland and also to the east over the Gulf of Maine and Atlantic Ocean near southern Nova Scotia. On several flights, sampling was done in the same general area as the Twin Otter, namely in the vicinity of the surface sampling site at Chebogue Point, Nova Scotia. Flight altitudes ranged from below 100 m to 6 km. Measurements made near the North American mainland showed evidence of nearby emission sources, whereas measurements made near southern Nova Scotia indicated, in general, an aged photochemical mixture.

3.2. Trace Gas Measurements: Twin Otter Data

Calculations were performed at 82 points from the Twin Otter flights for which there are measurements of hydrocarbons, O_3, and NO_y. In 65 cases, CO was also available; for the other 17 cases we relied on a correlation between CO and C_2H_2 (part 2):

$$CO\ (ppb) = 90.9 + 0.229\ C_2H_2\ (ppt),\ r^2 = 0.67 \qquad (1)$$

H_2O_2 was treated as a calculated compound because observations are relatively sparse and because this gives us a point of comparison between observed and calculated concentrations.

Ozone and water vapor mixing ratios are shown in Figure 1. Results from calculations will be presented for the four combinations of low and high O_3 and low and high water vapor that are shown on the figure. This division is motivated by an interest in high O_3 events and their difference in moist and dry air. Isoprene turns out to have a pronounced effect on the calculations. We therefore limit these four groups to samples having isoprene <0.1 ppb and create a fifth group with isoprene above 0.1 ppb. This value was selected as a breakpoint that reflected the bimodal distribution of isoprene concentration measurements. Group 5 had isoprene concentrations that ranged from 0.11 to 0.86 ppb, while groups 1-4 had all samples below 0.05 ppb and most below detection limit. In accord with the terrestrial biogenic source for isoprene, all group 5 samples were collected over or near land. The other four groups, with but a single exception, contain samples taken over coastal areas or over the open ocean. Figure 1 shows that high isoprene tends to occur in moist air masses with low O_3.

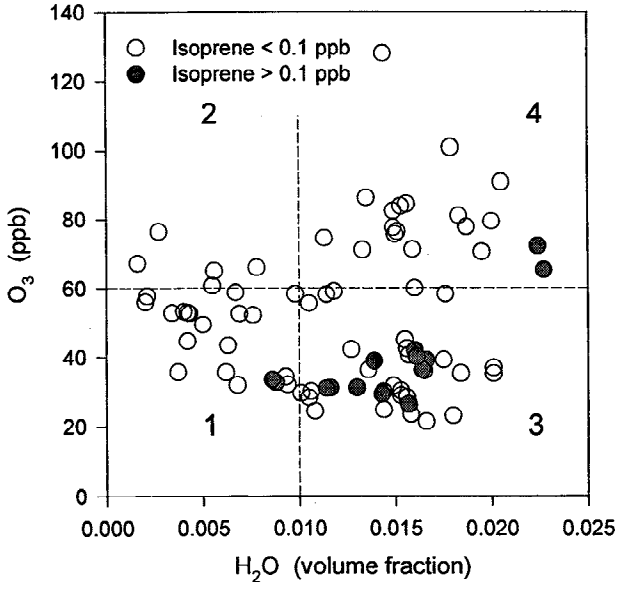

Figure 1. Scatter diagram showing O_3 and H_2O in 82 Twin Otter samples. Points with high isoprene (>0.1 ppb) are highlighted. Quadrants are labeled 1-4 with numbers corresponding to data subsets identified in Table 1.

Table 1. Summary of Calculations: Average Values for Input Parameters and Calculated Quantities as a Function of Composition Category

Variable	Data Subset 1	2	3	4	5
O_3, ppb	<60	>60	<60	>60	all
H_2O, vol mix ratio	<0.01	<0.01	>0.01	>0.01	all
Isoprene, ppb	<0.1	<0.1	<0.1	<0.1	>0.1
Number of samples	18	5	27	17	15
Input:					
Altitude, m	2818	2963	627	1282	529
Temperature, °C	6	7	17	16	19
H_2O, percent volume mising ratio	0.57	0.46	1.48	1.61	1.48
O_3, ppb	47	67	37	83	39
CO, ppb	122	164	131	223	122
Isoprene, ppb	0.00	0.00	0.01	0.00	0.39
NO_y, ppt	1000	2760	2050	7360	2910
NO, ppt	14	34	26	76	130
Calculated:					
NO_x, ppt	46	125	114	509	757
PAN, ppt	470	590	280	1650	1740
OH, 10^6 molecules cm^{-3}	2.8	4.0	3.4	6.8	2.9
HO_2, ppt	16	19	16	26	18
RO_2, ppt	12	9	13	16	25
HO_2+RO_2, ppt	28	28	29	42	43
$RO_2/(HO_2+RO_2)$	0.43	0.31	0.45	0.37	0.59
H_2O_2, ppb	1.9	2.1	3.1	5.1	3.8
ROOH, ppb	0.7	0.5	0.8	0.7	1.9
HCHO, ppb	0.34	0.44	0.65	1.2	3.5
Q, ppb h^{-1}	0.40	0.46	0.58	1.36	1.11
R+R, %	99	97	97	91	87
$R+NO_x$, %	1	3	3	9	13
$P(H_2O_2)$, ppb h^{-1}	0.08	0.10	0.14	0.33	0.18
P(ROOH), ppb h^{-1}	0.10	0.09	0.11	0.21	0.25
$P(O_3)$, ppb h^{-1}	0.23	0.53	0.53	2.09	4.02
$P\text{-}L(O_3)$, ppb h^{-1}	-0.004	0.19	0.22	1.14	3.64

Characteristics of the five data subsets are summarized in the top section of Table 1. This table reiterates the observations from part 1 and 2 that high O_3 events are associated with high concentrations of other anthropogenic pollutants and that these events are qualitatively different in dry and moist air masses.

Figure 2 indicates average composition as a function of altitude. Averages have been calculated for two data subsets. First, for the 67 low isoprene samples, 66 of which were collected over coastal areas or over the ocean. Second, we consider a larger and hopefully more climatologically significant data set, consisting of the entire over-water portion from all 48 Twin Otter flights. A comparison between the two sets of

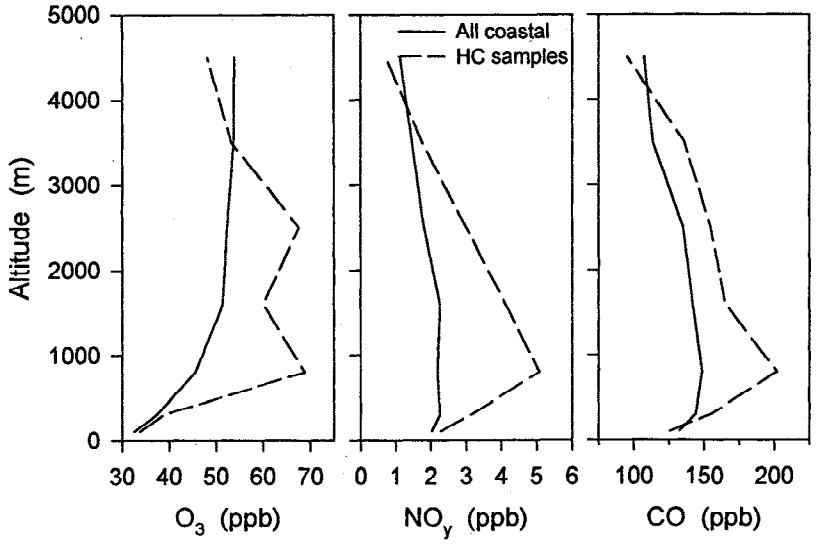

Figure 2. Vertical profiles for O_3, NO_y, and CO. Data were binned into the altitude ranges shown in Table 2. Solid lines indicate average concentrations determined from over-water flight segments from all 48 Twin Otter flights. Dashed lines are averages over the 67 low isoprene sample points.

vertical profiles indicates a bias in the hydrocarbon sampling whereby more samples were taken under polluted conditions. Although flights were conducted on 29 out of 34 days, and these 29 days were meteorologically representative of the entire experimental period [*Banic et al.*, 1996], there may still be a bias toward polluted conditions in the entire data set as multiple flights were conducted on O_3 episode days.

Although there were significant flight to flight variations in solar irradiance, we decided to use a nominal fixed value for our calculations in order to obtain radical concentrations and O_3 production rates which could be compared from one calculation to the next. The nominal solar irradiance was chosen to be a clear sky value based on flight notes indicating the prevalence of clear-sky conditions and measurements of upward and downward solar irradiance from the Twin Otter.

3.3. NO and NO_y - King Air Data

NO measurements are not available from the Twin Otter because of instrument problems described in part 1. Fortunately, there are NO measurements from the King Air taken under comparable conditions [*Buhr et al.*, 1996]. NO concentrations applicable to the Twin Otter samples have been obtained by multiplying the ratio NO/NO_y determined from the King Air by the NO_y concentration measured from the Twin Otter at the time that the hydrocarbon samples were collected.

NO to NO_y ratios were separately determined for the low and high isoprene subsets. Samples with low isoprene concentration (the first four categories in Table 1) were collected almost entirely over the Atlantic Ocean within 50 km of Chebogue Point. There were nine King Air flights in this region which were used to determine NO/NO_y as a function of NO_y for the four combinations of low and high O_3 and low and high dew point listed in Table 1. Flight segments below 200 m were excluded from this analysis as they had ratios of NO to NO_y that differed significantly from those found at higher altitude, perhaps indicating local effects of emission sources in Yarmouth. Differences between the four low isoprene subsets were relatively minor in comparison to the overall variability, and it was therefore decided to use a single relation between NO and NO_y as shown in Figure 3.

Samples with an isoprene concentration >0.1 ppb were collected over land, primarily near Kejimkujik National Park or Saint John, New Brunswick. A ratio could not be specifically determined for those regions because King Air flight time in those regions was very limited. Instead, results from the principal component analysis of *Buhr et al.* [1996] were used. Figure 10 of that study shows NO/NO_y as a function of NO_y for two data subsets. One subset consists of measurements which are dominated by a principal component that is representative of

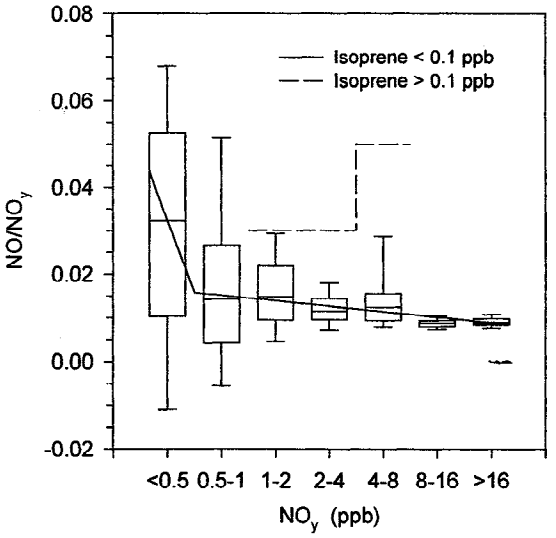

Figure 3. Ratio of NO to NO_y as a function of NO_y. Box plot shows the distribution of values observed near southern Nova Scotia from the King Air aircraft [*Buhr et al.*, 1996]. Whiskers indicate 10 and 90th percentile of distribution; box indicates 25 and 75th percentile and horizontal line for median. Solid line is the fit to the King Air data used in this study for low isoprene cases. For NO_y < 0.5 ppb, NO/NO_y = -0.0169-0.1088 log(NO_y (ppb)). For NO_y >0.5 ppb, NO/NO_y = 0.0144-0.0045 log(NO_y (ppb)). Dashed line indicates NO/NO_y used in high isoprene cases; NO/NO_y = 0.03 for NO_y < 4 ppb; NO/NO_y = 0.05 for NO_y >4 ppb. Span of solid and dashed lines corresponds approximately to range of NO_y in Twin Otter samples.

aged anthropogenically influenced O_3. NO/NO_y for that component is generally within 30% of the values determined from the King Air measurements near Chebogue Point. The other subset is dominated by a component that represents fresh emissions. Because many of the Twin Otter samples with isoprene concentration >0.1 ppb were collected near source regions, they are assumed to have a NO to NO_y ratio similar to that obtained for the King Air fresh emission subset. A minor simplification yields the relation identified in Figure 3 as applying to the high isoprene subset. At a given NO_y concentration, the amount of NO in the high isoprene samples is 2-5 times greater than in the low isoprene samples.

3.4. Hydrocarbon Reactivity

Hydrocarbon concentrations for C2 to C9 compounds were determined by gas chromatographic (GC) flame ionization analysis of samples collected in 6l pressurized containers as described in part 2. Reactivity of individual compounds was calculated as the product of concentration and rate constant for reaction with OH, evaluated at the temperature and pressure of the samples. Several of the more reactive species such as t-2-butene had background levels of unknown origin in the low parts-per-trillion (ppt) range. This background was nearly uniform among the cleanest samples. We treated the background as an artifact to be subtracted from the signal based on an expectation that concentrations of very reactive species should be near zero after several days travel time. Predictions from the photochemical calculations were insensitive to this subtraction.

Figure 4 shows the OH reactivity of CO, CH_4, isoprene, and nonisoprene hydrocarbons for five categories of samples. Reactivity is expressed as the rate of reaction of OH with each compound. A uniform concentration of 1700 ppb was assumed for CH_4. Variations between groups for CH_4+OH are due to differences in temperature. Except for the group with isoprene over 0.1 ppb, reactivity is dominated by CO and to a lesser extent CH_4. The contribution to reactivity from anthropogenic hydrocarbons is small in all cases. In as much as the oxidation pathways of CO and CH_4 are better understood than those of larger compounds, this feature facilitates our calculations.

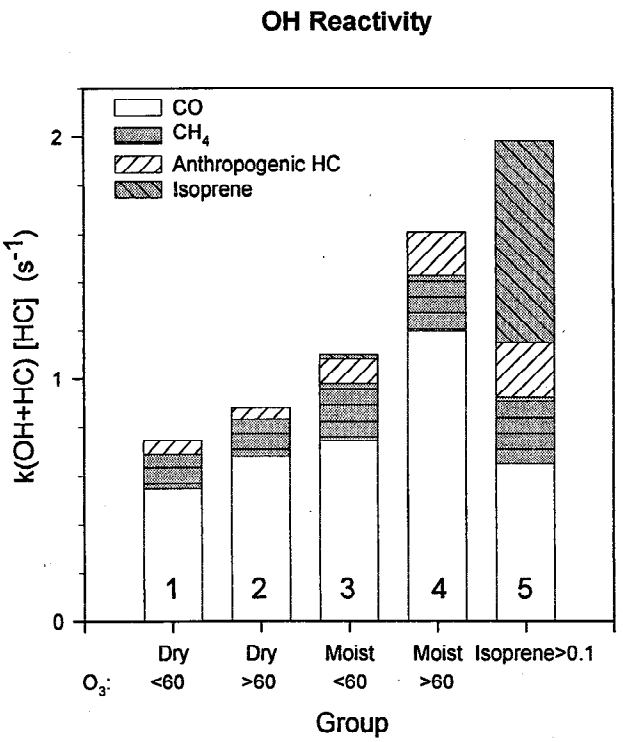

Figure 4. OH reactivity for five data subsets as shown on abscissa and as defined in Table 1. Reactivity is the product of concentration and rate constant for reaction with OH. See text for details.

4. Results

Calculations were done for the 82 Twin Otter samples using the chemical and physical measurements summarized in Table 1, the NO to NO_y ratios derived from King Air measurements, shown in Figure 3 and the hydrocarbon concentrations summarized in Figure 4. We will focus our attention on the 67 low isoprene samples that have characteristics of photochemically aged air that has been advected to Nova Scotia. In order to generate a more representative picture of O_3 formation and fast photochemistry in the region near Chebogue Point, an additional series of calculations was performed using the average concentrations and parameters determined from all coastal and over-water Twin Otter flight segments. For these calculations the average O_3, NO_y and CO shown in Figure 2 were combined with the average low isoprene HC concentrations.

For all of the calculations, photolysis rate constants are average values for the central 12 hours of daylight. Predicted concentrations and rates are approximately equal to an average value for 12 daylight hours. As photochemistry is much diminished at night, it can be assumed that the per day rate for production of radicals, peroxides, and O_3 is 12 times the daytime hourly average rate.

Tables 1 and 2 present an overview of the calculations with results averaged over composition category and over altitude bins. Note that the altitude bins include only low isoprene samples. Vertical profiles of $P(O_3)$ (O_3 production rate), $P-L(O_3)$ (net O_3 formation rate taking into account chemical loss), OH, HO_2+RO_2, H_2O_2, NO_x, and Q (radical production rate) are shown in Figures 5-11. Each figure shows the distribution of values that result from the individual Twin Otter samples, again eliminating the high isoprene cases. Comparison is made with model predictions that used chemical and meteorological data averaged over all 48 flights. Sensitivity calculations were done using an NO concentration that was halved or doubled. This perturbation caused a nearly proportional change to NO_x and $P(O_3)$. Radical concentrations were less affected; that is, a doubling of NO caused an average increase in OH of about 35% and a decrease in HO_2+RO_2 of about 10%.

The vertical profiles show a large variability in concentrations and rates at all altitudes except 4-5 km where there are only two samples. The variability is greatest between the surface and 2-3 km where, depending on wind flow, southern Nova Scotia can be exposed to pollutant plumes from urban or industrialized regions in North America. These plume samples constitute the moist, high O_3 subset in Table 1 and account for the high end of the frequency distributions for all of the quantities shown in Figures 5-11.

Although the moist plume samples have concentrations of O_3, NO_y, and CO that are characteristic of polluted environments, the concentrations of NO and NO_2 are low. In only four samples is NO_x above 0.5 ppb. In samples with low O_3, NO_x averages 46 and 114 ppt in dry and moist air, respectively. This feature is presumably due to over-water transport during which

Table 2. Summary of calculations: Average Values for Input Parameters and Calculated Quantities as a Function of Altitude Bin for Low Isoprene Samples

Variable	Altitude Range, m						
	0-200	200-400	400-1200	1200-2000	2000-3000	3000-4000	4000-5000
Number of samples	10	9	10	15	8	13	2
Input:							
Altitude, m	86	307	848	1456	2460	3145	4880
Temperature, °C	17	22	16	14	9	5	-6
H_2O, percent volume mixing nratio	1.49	1.70	1.52	1.22	0.93	0.61	0.49
O_3, ppb	34	39	69	60	68	53	48
CO, ppb	125	155	202	165	155	136	95
Isoprene, ppb	0.01	0.01	0.00	0.00	0.00	0.00	0.00
NO_y, ppt	2280	3160	5080	4130	3010	1760	730
NO, ppt	28	35	54	45	36	23	11
Calculated:							
NO_x, ppt	127	227	370	254	163	76	25
PAN, ppt	177	198	1020	1090	863	611	1150
OH, 10^6 molecules cm^{-3}	3.1	3.3	5.3	4.7	5.0	3.6	3.1
HO_2, ppt	14	17	22	20	21	18	16
RO_2, ppt	11	14	14	14	13	12	11
HO_2+RO_2, ppt	26	31	36	35	34	30	27
$RO_2/(HO_2+RO_2)$	0.44	0.47	0.39	0.42	0.38	0.39	0.41
H_2O_2, ppb	3.0	3.5	4.5	3.7	3.0	2.1	1.5
ROOH, ppb	0.7	0.9	0.7	0.8	0.6	0.7	0.6
HCHO, ppb	0.68	0.85	0.88	0.83	0.58	0.39	0.24
Q, ppb h^{-1}	0.50	0.68	1.05	0.89	0.78	0.48	0.36
R+R, %	97	96	93	95	96	98	99
$R+NO_x$, %	3	4	7	5	4	2	1
$P(H_2O_2)$, ppb h^{-1}	0.12	0.16	0.26	0.21	0.17	0.10	0.06
P(ROOH), ppb h^{-1}	0.09	0.13	0.16	0.16	0.15	0.11	0.10
$P(O_3)$, ppb h^{-1}	0.54	0.89	1.41	1.18	0.78	0.38	0.14
$P-L(O_3)$, ppb h^{-1}	0.28	0.51	0.68	0.61	0.24	0.08	-0.06

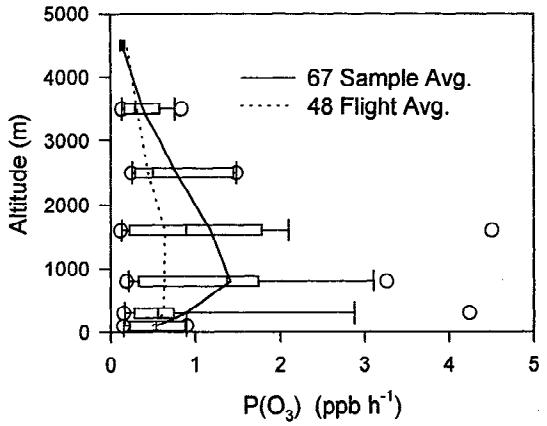

Figure 5. Vertical profile of O_3 production rate, $P(O_3)$; calculated as the rate of reaction of peroxy radicals with NO. Rate is an average value for 12 daytime hours. Box plot shows distribution of values for 67 low isoprene samples in altitude bins 0-200, 200-400, 400-1200, 1200-2000, 2000-3000, 3000-4000, and 4000-5000 m. Circles indicate points outside of the 10-90 percentile range. Whiskers indicate 10 and 90^{th} percentile. Box indicates 25-75^{th} percentile range with line for median. Solid line is an average for the 67 low isoprene samples, that is, the data depicted in the frequency distribution. Dotted line is an average calculated for the entire over-water portion of all 48 flights, a larger more representative data set than the 67 HC samples.

time there is oxidation of NO_x and no additional input of pollutants. Also, a stable temperature profile over the water leads to minimal deposition losses for NO_x oxidation products [*Daum et al.*, 1996]. As a consequence, the NO to NO_y ratio observed by *Buhr et al.* [1996] is relatively low as is the NO_x to NO_y ratio determined using calculated values for NO_2. For the

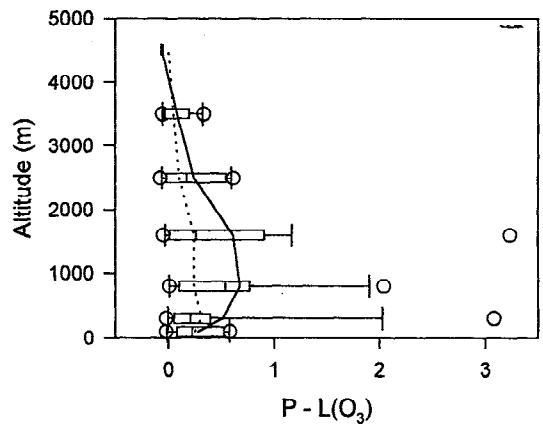

Figure 6. Vertical profile of net O_3 production rate taking into account chemical loss, $P-L(O_3)$. Loss of O_3 is due to photolysis, reaction with OH and HO_2, and reactions with olefins. Same format as figure 5.

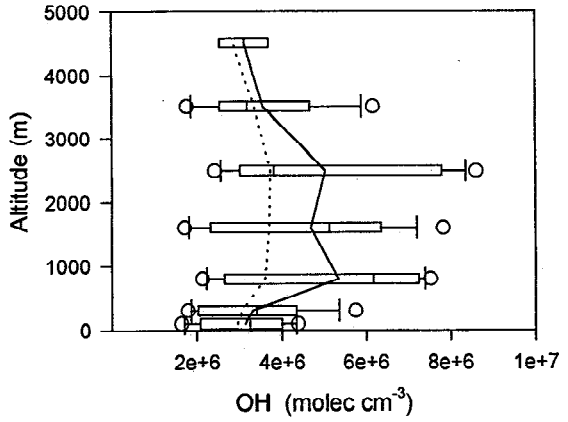

Figure 7. Vertical profile of OH. Same format as Figure 5.

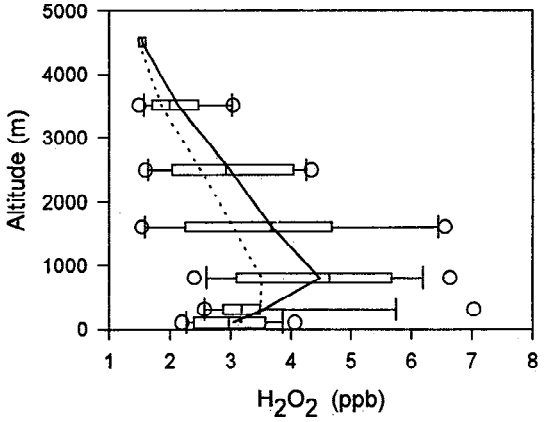

Figure 9. Vertical profile of H_2O_2. Same format as Figure 5.

samples in subsets 1-4, NO_x/NO_y ranges from 5 to 9% which is much lower than observed near emission sources [*National Research Council*, 1991; *Parrish et al.*, 1993]. It is also towards the low end of observed ratios at remote locations [*Atlas et al.*, 1992; *Carroll et al.*, 1992; *Sandholm et al.*, 1994; *Koike et al.*, 1996].

In the four low isoprene subsets, $P(O_3)$ varies from 0.1 to 4.5 ppb h^{-1} and P-$L(O_3)$ from -0.1 to 3.2 ppb h^{-1}. Vertical average (0-5000 m) values for $P(O_3)$ and P-$L(O_3)$ are 0.73 and 0.29 ppb h^{-1} for the 67 HC samples and 0.44 and 0.13 ppb h^{-1} for the average Twin Otter conditions. These rates are given as hourly averages for 12 hours of daylight, and so must be multiplied by 12 to get the daily change. In Table 3 we show O_3 production rates for two other layers, 0-200 m and 0-2000 m. These are compared with values for the eastern United States obtained from a modeling study by *McKeen et al.* [1991] and also compared with values derived from near-surface measurements at a rural site in Georgia [*Kleinman et al.*, 1995]. $P(O_3)$ and P-$L(O_3)$ are seen to be significantly higher over the eastern United States compared with Nova Scotia. This is particularly true near the surface where continental sites are exposed to fresh NO_x emissions. As discussed in a following section, the relatively low production rate for O_3 near southern Nova Scotia is mostly caused by low NO. We also note that sample to sample differences in $P(O_3)$ are due in large part to differences in NO.

The samples with the highest average $P(O_3)$ and P-$L(O_3)$ are the high isoprene subset which is not included in Figures 5-11. For these samples, high $P(O_3)$ is partially due to isoprene itself and partially due to the higher NO fraction that was assumed. Though P-$L(O_3)$ is predicted to average 3.6 ppb h^{-1}, or 44 ppb d^{-1}, in the high isoprene sample, O_3 is relatively low. This may be a consequence of an overestimate of NO or a reflection of near-source sampling whereby O_3 has not had a chance to form and may never reach high values due to dilution as the air mass is advected away.

5. Discussion

5.1. Low NO_x Photochemistry: O_3 Production and Sources and Sinks of Radicals

A defining characteristic of the Twin Otter samples is that NO_x levels are low. Consequences of low NO_x (and definitions of what constitutes low NO_x and high NO_x conditions) have been discussed by *Kleinman* [1994] and *Sillman et al.* [1990] and *Sillman* [1995]. The definition that will be used here is that low NO_x conditions occur when radical removal is dominated by radical-radical processes such as $HO_2 + HO_2$ or $HO_2 + RO_2$. In contrast, high NO_x conditions exist when the dominant radical removal process is radical + NO_x, exemplified by $OH+NO_2$.

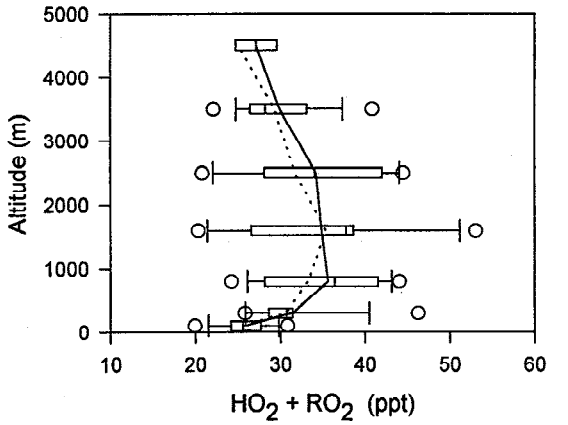

Figure 8. Vertical profile of peroxy radical concentrations, HO_2+RO_2. Same format as Figure 5.

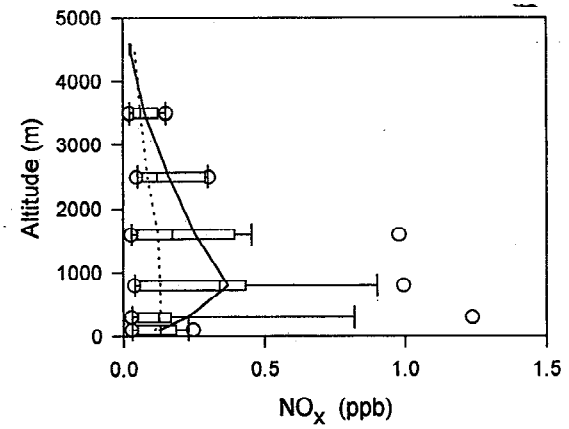

Figure 10. Vertical profile of NO_x (NO + NO_2). Same format as Figure 5.

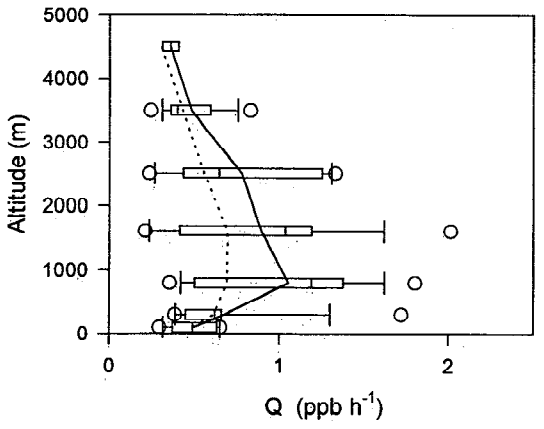

Figure 11. Vertical profile of radical production rate, Q. Same format as Figure 5.

These two major radical removal pathways will be abbreviated as R+R and R+NO_x. We keep track of radical production and destruction processes by adding counter species to the chemical mechanism. Tables 1 and 2 indicate the production rate of radicals, Q, (also shown in Figure 11) and the fraction of radicals removed by R+R or R+NO_x. In the low isoprene subsets, R+R accounts for 91-99% of the total removal, qualifying these sample as being low NO_x.

Under low NO_x conditions a budget equation can be written for radicals which yields an O_3 production rate [*Kleinman et al.*, 1994, 1995]:

$$P(O_3) = k_3\, Q^{1/2}/(2\, k_{eff})^{1/2}\, [NO] \qquad (2)$$

where k_3 is the rate constant for HO_2 (or RO_2) + NO → NO_2, k_{eff} is an effective rate constant for peroxide formation given by

$$k_{eff} = k_1(1 - \alpha)^2 + k_2(1 - \alpha)\alpha \qquad (3)$$

$$\alpha = [RO_2]/([HO_2]+[RO_2]) \qquad (4)$$

and k_1 and k_2 are rate constants for the similarly numbered reactions

(R1) $\quad 2\, HO_2 \rightarrow H_2O_2$

(R2) $\quad HO_2 + RO_2 \rightarrow ROOH$

Although in this study we do not have to rely on (2) to determine $P(O_3)$, the utility of this equation is that $P(O_3)$ is expressed in terms of quantities that can be readily measured or (in the case of k_{eff}) estimated.

According to (2), $P(O_3)$ should be proportional to $Q^{1/2}[NO]$. This relation is tested in Figure 12. For either the linear or log quantities, 99% of the variance in $P(O_3)$ is explained by $Q^{1/2}[NO]$. The scatter in Figure 12 is mostly due to sample to sample variations in k_{eff} caused by varying fractions of HO_2 and RO_2 radicals. There is also a slight breakdown of the low NO_x condition in samples with high isoprene in which a high NO to NO_y ratio has been assumed. Most of the variability in $Q^{1/2}[NO]$ is due to changes in [NO] which varies from 8 to 135 ppt in low isoprene samples and from 18 to 384 ppt in high isoprene samples. As a consequence, [NO] alone can explain 93% of the variance in $P(O_3)$.

The current data set does not permit a true evaluation of (2) as we have no independent way of determining $P(O_3)$. The correlation of the data in Figure 12, however, demonstrates that the low NO_x approximation is valid for our Twin Otter samples. In a previous study conducted using measurements from a surface site in the rural southeastern United States, we were able to compare $P(O_3)$ from (2) with a photostationary state calculation [*Kleinman et al.*, 1995]. An error analysis of both techniques indicated agreement between these methods to the extent permitted by their respective measurement uncertainties.

Another consequence of low NO_x conditions is that the formation rate for peroxide should be proportional to Q, the radical production rate. This relation serves as the basis for comparing observed concentrations of H_2O_2 or total peroxide with various measures of radical production rate [see, e.g., *Daum et al.*,1990; *Tremmel et al.*, 1993; *Slemr and Tremmel*, 1994; *Dommen et al.*, 1995; *Weinstein-Lloyd*, 1996]. In as much as the primary source of radicals is often short wavelength photolysis of O_3 followed by reaction of $O(^1D)$ with H_2O, peroxide concentration is found to be correlated with O_3, H_2O, dew point, or the product of H_2O times O_3. A major assumption

Table 3. Vertical Averages for O_3 Production Rate, $P(O_3)$, and Net Production Rate, $P\text{-}L(O_3)$

Data Set	Altitude Range, m		
	0-200[a]	0-2000[b]	0-5000
$P(O_3)$ ppb h^{-1}			
NARE low isoprene	0.54	1.2	0.73
NARE average[c]	0.50	0.62	0.44
Eastern United States[d]	5.4	2.2	
Metter, Georgia[e]	4.7		
$P\text{-}L(O_3)$ ppb h^{-1}			
NARE low isoprene	0.28	0.59	0.29
NARE average[c]	0.24	0.25	0.13
Eastern United States[d]	2.7	0.9	
Metter, Georgia[e]	4.2		

[a]0-75 m for eastern United States; near surface for Metter, Georgia.
[b]0-1800 m for eastern United States.
[c]Over-water portion of all 48 Twin Otter flights.
[d]From *McKeen et al.* [1991, Figure 11].
[e]From radical budget calculation of *Kleinman et al.* [1995].

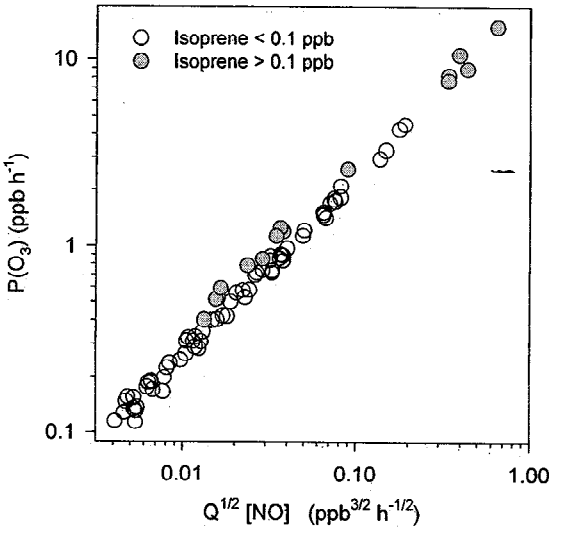

Figure 12. Dependence of $P(O_3)$ on $Q^{1/2}$ [NO] for all Twin Otter samples from model calculations. A linear relation is predicted from equation (2).

is that peroxide concentration is proportional to its production rate.

In Figure 13 we show predicted H_2O_2 as a function of Q. A linear least squares fit to these calculated points yields the following relation:

$$H_2O_2 \text{ (ppb)} = 1.18 + 2.74 \text{ Q (ppb h}^{-1}\text{)}, \quad r^2 = 0.85 \qquad (5)$$

The data are well represented by a straight line but, as with the NARE H_2O_2 measurements from the G-1 reported by *Weinstein-Lloydet al.* [1996], there is a positive intercept so that $[H_2O_2]/Q$ is higher at low Q. This is equivalent to the lifetime of H_2O_2 becoming longer as Q decreases in dry and/or clean air. Loss of H_2O_2 is due in part to reaction with OH and Table 1 indicates that OH decreases in dry-clean air relative to moist-dirty air.

5.2. H_2O_2 Observations

H_2O_2 measurements from the Twin Otter were briefly described in part 1 and are presented in detail by J. Weinstein-Lloyd et al. (manuscript in preparation, 1996). A comparison with coincident calculated H_2O_2 is shown in Figure 14. The observations in Figure14 have been screened to eliminate data points where loss due to wet or dry deposition is expected, as these processes are not included in the calculation. Observed vertical profiles for H_2O_2 typically showed a lower concentration in the surface inversion layer relative to higher altitude, ranging from tens of percent to a factor of 2 or more. In spite of the stable atmosphere over the ocean, this decrease appeared to be associated with a surface (or near-surface) loss mechanism. We therefore restricted Figure 14 to samples from above 400 m. In order to reduce the likelihood of wet processing we also required that dew point depression be greater than 2°C and that FSSP number concentration (a measure of cloud droplets) be less than 10 cm^{-3}. Figure 14 also does not include data taken prior to flight 22. There was a large change in calibration factor between flights 21 and 22 associated with maintenance that was done when the instrument was removed from the Twin Otter. While there is no a priori reason to disregard data from before flight 22, we note that after flight 22 the measurements are better behaved in several ways. There is

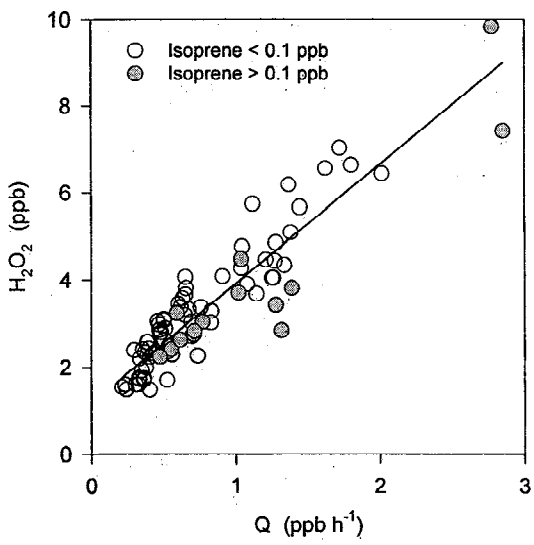

Figure 13. Dependence of H_2O_2 on Q for all Twin Otter samples from model calculations.

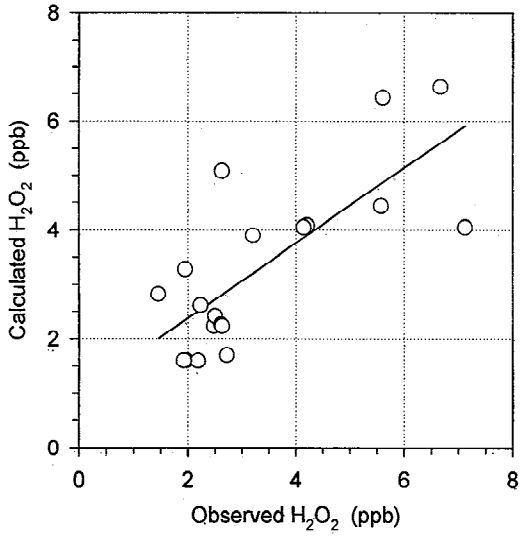

Figure 14. Comparison between calculated and observed H_2O_2. Data set screened as described in text to remove samples most affected by dry deposition and samples before flight 22.

better agreement with radical production rates and an improved comparison with the G-1 data set [*Weinstein-Lloyd* et al., 1996].

The 19 remaining observations have an r^2 correlation with calculated values of 0.57. Average calculated H_2O_2 is 1% lower than observed. Some of the differences are presumably due to the generic nature of the calculations using average photolysis rate constants and average NO to NO_y ratios. We also note that the timescale for H_2O_2 production can be several days in the dryer air masses and the neglect of history effects will introduce errors in our calculations.

6. Conclusions

Photochemical model calculations have been performed for the summer 1993 NARE intensive using trace gas observations from the Twin Otter and King Air aircraft as constraints. Calculations were done for two groups of samples having low or high isoprene concentration. The low isoprene group consists of locations over the ocean near southern Nova Scotia, whereas the high isoprene group contains sample points over land. The low isoprene samples were further subdivided based on O_3 and H_2O concentrations. Results are presented by data subset and for the low isoprene samples as vertical profiles. An altitude range from below 100 m to 5 km was covered. The calculations yield predictions for radical concentrations, oxidation products, chemical rates of change, and reaction pathway information. These predictions are based on average NO/NO_y ratios because NO measurements are not coincident with the other trace gas data.

Previous studies have indicated that polluted boundary layer air from the North American mainland can be advected out to Nova Scotia bringing high concentrations of O_3, NO_y, CO, and aerosol particles [*Banic et al.*, 1996; *Berkowitz et al.*, 1995; *Buhr et al.*, 1996; *Daum et al.*, 1996; *Kleinman et al.*, 1996a,b; *Leaitch et al.*, 1996]. Although these air masses resemble urban pollution in some respects, there is clear evidence that extensive photochemical processing has occurred during transport. Concentrations of reactive hydrocarbons are low; reactivity

toward OH is dominated by CO and CH_4 in all of the over-water samples. NO concentrations are also low as indicated by the King Air observations reported by *Buhr et al.* [1996]. This data set, which was used in our calculations, indicates that near southern Nova Scotia, the ratio of NO to NO_y varied from approximately 3% at low NO_y to 1% at high NO_y. Using calculated values for NO_2, we find that the ratio of NO_x to NO_y is lower than observed in many remote regions. NO_x/NO_y was only 7% in the data subset most closely associated with polluted boundary layer air.

Ozone production rates over southern Nova Scotia are calculated to be relatively low in comparison to average values for the eastern United States. For example, *McKeen et al.* (1991) calculate an average boundary layer (0-1800 m) O_3 production rate for the eastern United States of 2.2 ppb per daylight hour (multiply by 12 to get daily averages). The corresponding figure for southern Nova Scotia is 0.6 ppb h^{-1}. Taking into account chemical loss of O_3, *McKeen et al.* calculate a net production rate of 0.9 ppb h^{-1}; the corresponding NARE value is 0.25 ppb h^{-1}. This factor of 4 difference is partly due to the combination of continental and marine air masses that arrive in Nova Scotia and partly due to over-water transport in which NO_x is removed by oxidation and not replaced by fresh emissions.

There is considerable variation among the individual NARE samples as to O_3 production. Samples with low O_3 (<60 ppb) in dry air have an average net production rate that is slightly negative, whereas samples with high O_3 in moist air have an average net production rate of 1.1 ppb h^{-1}, comparable to the eastern United States average. Highest production rates occur in the high isoprene samples which were collected over land and therefore not included in determining average values for coastal southern Nova Scotia.

Relations between O_3 production rates and precursor concentrations are discussed in the context of the prevailing low NO_x conditions. We show that over 90% of radicals are removed by radical-radical reactions, and therefore, according to a low NO_x radical budget argument, $P(O_3)$ is proportional to $Q^{1/2}$ [NO], where Q is the radical formation rate. This relation explains 99% of the variance in the calculated $P(O_3)$. [NO] by itself explains over 93%. Predicted concentrations for H_2O_2 are well correlated with Q as expected for low NO_x conditions. A comparison between calculated and observed H_2O_2 indicates good agreement between average concentrations with a scatter ($r^2 = 0.57$ for a linear least squares regression) that is partly due to the use of diurnal average photolysis rate constants and an average NO to NO_y ratio.

Acknowledgments. The authors gratefully acknowledge a job well done by the ground and flight crews of the NRC Twin Otter. The many contributions of Steve Bacic, Catharine Banic, George Isaac, and Richard Leaitch of AES and Paul Klotz, Dan Leahy, Linda Nunnermacker, and Xianliang Zhou of BNL to the measurement campaign are gratefully acknowledged. A special thanks to Mark Couture of AES for help in data processing. We would like to thank the personnel at Yarmouth Airport for their hospitality and expert assistance. We also appreciate the accurate weather forecasts provided by AES at Yarmouth. This study was supported by funds from AES, NOAA, and the Atmospheric Chemistry Program of DOE. This paper has been authored under contract DE-AC02-76CH00016 with the U.S. Department of Energy under the Atmospheric Chemistry Program within the Office of Health and Environmental Research. Accordingly, the U.S. Government retains a nonexclusive, royalty free license to publish or reproduce the published form of this contribution or to allow others to do so for U.S. Government purposes.

References

Angevine, W.M., and J.I. MacPherson, Comparison of wind profiler and aircraft wind measurements at Chebogue Point, Nova Scotia, *J. Atmos. Oceanic Technol., 12*, 421-426, 1995.

Atlas, E.L., B.A. Ridley, G. Hübler, J.G. Walega, M.A. Carroll, D.D. Montzka, B.J. Huebert, R.B. Norton, F.E. Grahek, and S. Schauffler, Partitioning and budget of NO_y during the Mauna Loa Observatory Photochemistry Experiment, *J. Geophys. Res., 97*, 10,449-10,462, 1992.

Banic, C.M., W.R. Leaitch, G.A. Isaac, M.P. Couture, L.I. Kleinman, S.R. Springston, and J.I. MacPherson, Horizontal transport of ozone and sulphur during the North Atlantic Regional Experiment, *J. Geophys. Res., 101*, 29,091-29,104, 1996.

Berkowitz, C.M., K.M. Busness, E.G. Chapman, J.M. Thorp, and R.D. Saylor, Observations of depleted ozone within the boundary layer of the western North Atlantic, *J. Geophys. Res., 100*, 11,483-11,496, 1995.

Buhr, M., D. Sueper, M. Trainer, P. Goldan, B. Kuster, F. Fehsenfeld, G. Kok, R. Shillawski, and A. Schanot, Trace gas and aerosol measurements over the Gulf of Maine during the North Atlantic Regional Experiment (NARE 1993), *J. Geophys. Res., 101*, 29,013-29,027, 1996.

Cantrell, C.A., et al., Peroxy radicals in the ROSE experiment: Measurement and theory, *J. Geophys. Res., 97*, 20,671-20,686, 1992.

Cantrell, C.A., et al., Peroxy radicals as measured in ROSE and estimated from photostationary state deviations, *J. Geophys. Res., 98*, 18,355-18,366, 1993.

Carroll, M.A., B.A. Ridley, D.D. Montzka, G. Hubler, J.G. Walega, R.B. Norton, B.J. Huebert, and F.E. Grahek, Measurements of nitric oxide and nitrogen dioxide during the Mauna Loa Observatory Photochemistry Experiment, *J. Geophys. Res., 97*, 10,361-10,374, 1992.

Chameides, W.L., et al., Observed and model-calculated NO_2/NO ratios in tropospheric air sampled during the NASA GTE/CITE-2 field study, *J. Geophys. Res., 95*, 10,235-10,247, 1990.

Chylek, P., C.M. Banic, B. Johnson, P.A. Damiano, G.A. Isaac, W.R. Leaitch, P.S.K. Liu, F.S. Boudala, B. Winter, and D. Ngo, Black carbon: Atmospheric concentrations and cloud water content over southern Nova Scotia, *J. Geophys. Res., 101*, 29,105-29,110, 1996.

Crawford, J., et al., Photostationary state analysis of the NO_2-NO system based on airborne observations from the western and central North Pacific, *J. Geophys. Res., 101*, 2053-2072, 1996.

Daum, P.H., L.I. Kleinman, A.J. Hills, A.L. Lazrus, A.C.D. Leslie, K. Busness, and J. Boatman, Measurement and interpretation of concentrations of H_2O_2 and related species in the upper Midwest during summer, *J. Geophys. Res., 95*, 9857-9871, 1990.

Daum, P.H., L.I. Kleinman, L. Newman, W.T. Luke, J. Weinstein-Lloyd, C.M. Berkowitz, and K. Busness, Measurements of the chemical and physical properties of plumes of anthropogenic pollutants transported over the North Atlantic during the North Atlantic Regional Experiment, *J. Geophys. Res., 101*, 29,029-29,042, 1996.

Davis, D.D., et al., A photostationary state analysis of the NO_2-NO system based on observations from the subtropical/tropical North and South Atlantic, *J. Geophys. Res., 98*, 23,501-23,523, 1993.

Dommen, J., A. Neftel, A. Sigg, and D.J. Jacob, Ozone and hydrogen peroxide during summer smog episodes over the Swiss Plateau: Measurements and model simulations, *J. Geophys. Res., 100*, 8953-8966, 1995.

Eisele, F.L., G.H. Mount, F.C. Fehsenfeld, J. Harder, E. Marovich, D.D. Parrish, J. Roberts, M. Trainer, and D. Tanner, Intercomparison of tropospheric OH and ancillary trace gas measurements at Fritz Peak Observatory, Colorado, *J. Geophys. Res., 99*, 18,605-18,626, 1994.

Jacob, D.J., et al., Summertime photochemistry of the troposphere at high northern latitudes, *J. Geophys. Res., 97*, 16,421-16,431, 1992.

Kleinman, L.I., Low and high NO_x tropospheric photochemistry, *J. Geophys. Res., 99*, 16,831-16,838, 1994.

Kleinman, L, et al., Ozone formation at a rural site in the southeastern United States, *J. Geophys. Res., 99*, 3469-3482, 1994.

Kleinman, L., Y.-N. Lee, S.R. Springston, J.H. Lee, L. Nunnermacker, J. Weinstein-Lloyd, X. Zhou, and L. Newman, Peroxy radical concentration and ozone formation rate at a rural site in the southeastern United States, *J. Geophys. Res., 100*, 7263-7273, 1995.

Kleinman, L.I., P.H. Daum, Y.-N. Lee, S.R. Springston, L. Newman, W.R. Leaitch, C.M. Banic, G.A. Isaac, and J.I. MacPherson,

Measurement of O_3 and related compounds over southern Nova Scotia, Part 1, Vertical distributions, *J. Geophys. Res.*, *101*, 29,043-29,060, 1996a.

Kleinman, L.I., P.H. Daum, S.R. Springston, W.R. Leaitch, C.M. Banic, G.A. Isaac, T. Jobson, and H. Niki, Measurement of O_3 and related compounds over southern Nova Scotia, Part 2, Photochemical age and vertical transport, *J. Geophys. Res.*, *101*, 29,061-29,074, 1996b.

Koike, M., Y. Kondo, S. Kawakami, H.B. Singh, H. Ziereis, and J.T. Merill, Ratios of reactive nitrogen species over the Pacific during PEM-West A, *J. Geophys. Res.*, 101, 1829-1851, 1996.

Leaitch, W.R., C.M. Banic, G.A. Isaac, M.D. Couture, P.S.K. Liu, I. Gultepe, S.-M. Li, L. Kleinman, P.H. Daum, and J.I. MacPherson, Chemical and physical observations in marine stratus during NARE 1993: Factors controlling cloud droplet number concentrations, *J. Geophys. Res.*, *101*, 29,123-29,135, 1996.

Lee, Y.-N., X. Zhou, W.R. Leaitch, and C.M. Banic, An aircraft measurement technique for formaldehyde and soluble carbonyl compounds, *J. Geophys. Res.*, *101*, 29,075-29,080, 1996.

Li, S.-M., C.M. Banic, W.R. Leaitch, P.S.K. Liu, G.A. Isaac, X.-L. Zhou and Y.-N. Lee, Water-soluble fractions of aerosol and their relations to number size distributions based on aircraft measurements from the North Atlantic Regional Experiment, *J. Geophys. Res.*, *101*, 29,111-29,121, 1996.

Liu, S.C., et al., A study of the photochemistry and ozone budget during the Mauna Loa Observatory Photochemistry Experiment, *J. Geophys. Res.*, *97*, 10,463-10,471, 1992.

Madronich, S., Photodissociation in the atmosphere, 1, Actinic flux and the effects of ground reflections and clouds, *J. Geophys. Res.*, *92*, 9740-9752, 1987.

McKeen, S.A., E.Y. Hsie, M. Trainer, R. Tallamraju, and S.C. Liu, A regional model study of the ozone budget in the eastern United States, *J. Geophys. Res.*, *96*, 10,809-10,845, 1991.

National Research Council, *Rethinking the Ozone Problem in Urban and Regional Air Pollution*, Natl. Acad. Press, Washington, D. C., 1991.

Parrish, D.D., et al., The total reactive oxidized nitrogen levels and the partitioning between the individual species at six rural sites in eastern North America, *J. Geophys. Res.*, *98*, 2927-2939, 1993.

Paulson, S.E., and J.H. Seinfeld, Development and evaluation of a photochemical mechanism for isoprene, *J. Geophys. Res.*, *97*, 20,703-20,715, 1992.

Poppe, D., et al., Comparison of measured OH concentrations with model calculations, *J. Geophys. Res.*, *99*, 16,633-16,642, 1994.

Ridley, B.A., S. Madronich, R.B. Chatfield, J.G. Walega, R.E. Shetter, M.A. Carroll, and D.D. Montzka, Measurements and model simulations of the photostationary state during the Mauna Loa Observatory Experiment: Implications for radical concentrations and ozone production and loss rates, *J. Geophys. Res.*, *97*, 10,375-10,388, 1992.

Sandholm, S., et al., Summertime partitioning and budget of NO_y compounds in the troposphere over Alaska and Canada: ABLE 3B, *J. Geophys. Res.*, *99*, 1837-1861, 1994.

Sillman, S., The use of NO_y, HCHO, H_2O_2, and HNO_3 as indicators for ozone-NO_x-hydrocarbon sensitivity in urban locations, *J. Geophys. Res.*, *100*, 14,175-14,188, 1995.

Sillman, S., J.A. Logan, and S.C. Wofsy, The sensitivity of ozone to nitrogen oxides and hydrocarbons in regional ozone episodes, *J. Geophys. Res.*, *95*, 1837-1851, 1990.

Slemr, F. and H.G. Tremmel, Hydroperoxides in the marine troposphere over the Atlantic Ocean, *J. Atmos. Chem.*, *19*, 371-404, 1994.

Stockwell, W.R., P. Middleton, J.S. Chang, and X. Tang, The second generation regional acid deposition model chemical mechanism for regional air quality modeling, *J. Geophys. Res.*, *95*, 16,343-16,367, 1990.

Tremmel, H.G., W. Junkermann, F. Slemr, and U. Platt, On the distribution of hydrogen peroxide in the lower troposphere over the northeastern United States during late summer 1988, *J. Geophys. Res.*, *98*, 1083-1099, 1993.

Weinstein-Lloyd, J., P.H. Daum, L.J. Nunnermacker, J.H. Lee, and L.I. Kleinman, Measurement of peroxides and related species in the 1993 North Atlantic Regional Experiment, *J. Geophys. Res.*, *101*, 29,081-29,090, 1996.

M. Buhr and B. T. Jobson, Aeronomy Laboratory, National Oceanic and Atmospheric Administration, Boulder, CO 80303.

P. H. Daum, L. I. Kleinman, J. H. Lee, Y.-N. Lee, S. R. Springston, and J. Weinstein-Lloyd, Brookhaven National Laboratory, Department of Applied Science, Environmental Chemistry Division, Upton, NY 11973-5000. (e-mail: phdaum@bnl.gov; kleinman@bnl.gov; jaihlee@bnl.gov; ynlee@bnl.gov; srs@bnl.gov; jlloyd@bnl.gov.)

(Received January 6, 1997; revised May 14, 1997;
accepted May 16, 1997.)